Journal of Applied Polymer Science

Evaluation of high temperature polymers in nanolayered films and gradient refractive index (GRIN) lenses

Kezhen Yin,[1] Shanzuo Ji,[1] Howard Fein,[2] Michael Ponting,[2] Andrew Olah,[1] Eric Baer[1]

[1]Case Western Reserve University, Center for Layered Polymeric Systems, Department of Macromolecular Science and Engineering, 2100 Adelbert Road, Cleveland, Ohio 44106

[2]PolymerPlus LLC, 7700 Hub Parkway, Valley View, Ohio 44125

Correspondence to: K. Yin (E-mail: kxy77@case.edu)

ABSTRACT: A new polymer nanolayer gradient refractive index (GRIN) system with more robust thermal stability because of incorporation of a high glass transition temperature polyester, OKP4HT, was demonstrated. A combination of extruded nanolayered GRIN film systems, comprised of five unique polymer materials, were combined to produce laminate optics comprised of a large internal refractive index gradient distribution, $n = 1.445 - 1.630$, without degradation of optical transmissive properties. The optical performance of a series of varied magnitude GRIN lenses, ranging from $\Delta n = 0$ to 0.185, was evaluated. Increasing the lens refractive index range resulted in decreased optic sphericalaberrations that followed analytical predictions. An analytical approach was reported to correlate the polymer material upper service temperature (UST) to the onset of polymer material loss modulus as measured by DMTA. Thermo-optical interferometry measurements of irreversible lens deformation confirmed the lenses UST at 125°C for the OKP4HT/PC system as compared to 75°C for a PMM/SAN17 system. © 2015 Wiley Periodicals, Inc. J. Appl. Polym. Sci. **2015**, *132*, 42741.

KEYWORDS: biomimetic; extrusion; property relations; structure

Received 15 April 2015; accepted 16 July 2015

DOI: 10.1002/app.42741

INTRODUCTION

Optical grade polymers have been widely used in many optical products and applications, including charge-coupled device (CCD) cameras,[1] prisms,[2] laser collimation,[3] sensors,[4] medical disposal optics,[5] and optical fibers.[6] Polymer materials have advantages as compared with traditional inorganic glasses which include lower material density, better impact resistance, and ease of mass producibility/lower cost. Polymer materials are generally between one half and one fifth of the densities of comparable inorganic glass. The cost of injection/compression molding and polishing of precision polymer optical devices is cheaper and less time-consuming than that of grinding and polishing glass devices, which offers higher volume production capabilities that are fast, repeatable, and lower cost. Polymer materials also possess higher impact properties and avoid fracture/chipping much better than glass that leads to optical lens durability in high vibration or impact optics for military applications like goggles, vehicle optics, and heads-up displays.[1,7]

However, current optical grade polymers materials have certain drawbacks which limit their application as compared to inorganic glasses. Polymer optical devices have lower environmental exposure conditions, i.e. temperature/humidity/radiation, as compared with inorganic glass. Another disadvantage of polymer optical devices is attributed to its relatively lower refractive index/optical power associated with polymer.[8] To overcome these drawbacks, an emerging polyester-based polymer (OKP4HT, Osaka Gas Chemical) has been developed with a glass transition temperature of 142°C and refractive index of 1.63. This material also has extremely low birefringence and is highly transmissive in the visible and SWIR wavelengths.

Availability of a high refractive index, high temperature resistant optical polymer material like OKP4HT enables potential advances in specialty polymer optics enabling performance and plastic lens inclusion into environments and optical systems were environmental conditions require material survivability above 100°C.[9] Incorporation of the OKP4HT material into nanolayered polymer gradient refractive index (GRIN) lenses is an approach that would benefit from the higher material refractive index and operation temperatures. An alternative way to improve the performance of polymer optical devices is based on advanced processing methodology. Polymeric GRIN lenses, fabricated through a process of nanolayer coextrusion and film lamination,[10,11] have demonstrated high optical performance and lightweight designs through utilization of a variety of axial, radial, and spherical GRIN profiles, large refractive index differences, and lens apertures.[12–14]

Table I. Materials for High Δn GRIN Lens

Material	Commercial name	R.I. @633 nm	T_g (°C)	Melting point (°C)	Films extrusion temperature (°C)
OKP4HT	OKP4HT (Fiber Optics)	1.63	142	-	250
PC	Calibre 201-15 (Styron)	1.58	147	-	250
SAN17	Lustron (Ineos)	1.57	104	-	230
PMMA	Plexiglas V920 (Arkema)	1.49	99	-	230
PVDF-HFP	Solef 21508 (Solvay)	1.40	−29	135	230

The purpose of this work is to evaluate the performance of high temperature polymer, OKP4HT, processed with nanolayer coextrusion for optical applications. The extension of optical polymer materials, and polymeric GRIN lenses, to include environmental conditions and device service temperatures greater than 75°C is advantageous for space and military issued devices. Polymer nanolayered films with OKP4HT were extruded using nanolayer coextrusion techniques. The refractive index and light transmission of the films were confirmed. One of the motivations to develop nanolayer GRIN systems was to achieve better optical performance because of its high refractive index. A series of plano-convex lenses were produced with varied magnitudes of GRIN distributions, ranging from 0 to 0.185, through incorporation of OKP4HT/Polycarbonate (PC) with poly(methyl methacrylate) (PMMA)/ Styrene–acrylonitrile copolymer (SAN17) nanolayers. The effect of OKP4HT inclusion into nanolayered, polymeric GRIN lenses was evaluated through measurements of the lens optical power and interferometric surface measurements to GRIN lens geometry as a function of cyclic exposure to hot/cold temperature environments. Thermal hysteresis measurements were used to recommend the upper service temperature, i.e. high temperature exposure limit, of a PC/OKP4HT GRIN lens and a PMMA/SAN17 GRIN lens. The effect of temperature on the OKP4HT polymer material was also correlated with thermal mechanical properties of polymer nanolayer films.

EXPERIMENTAL

Materials

High temperature polyester, was supplied by the Osaka Gas Chemicals (Angstromlink AL-6263). Polycarbonate was supplied by The Dow Chemical Company (PC, Calibre 201-15). Styrene–acrylonitrile copolymer was provided by Bayer Cooperation (SAN17, Lustran Sparkle) with 17 wt % of acrylonitrile in the copolymer.[15] Poly(methyl methacrylate) was provided by Arkema (PMMA, Plexiglas V920). Poly(vinylidene fluoride-co-trifluoroethylene) was provided by Solvay Plastics (PVDF-HFP, Solef 21508). All resins were used "as-received" without further purification or modification. A PVDF-blend (PVDFb) was produced by extrusion blending PMMA with PVDF-HFP (1 : 1 v/v) at 230°C using a Haake 18 mm twin screw extruder. The optical and thermal properties of these materials are listed in Table I.

Polymer Nanolayer Film Extrusion

Polymer nanolayered films were processed via a forced assembly film coextrusion processing technique at Case Western Reserve University.[16] The setup of this continuous processing unit to produce nanolayered films was illustrated in Figure 1. In forced assembly coextrusion, two polymer materials, A and B, were extruded via two single-screw extruders at a matched viscosity extrusion temperature followed with conveyance into the layering dies by two melt metering pumps. The metering pumps were used to ensure a desired volumetric ratio of polymer A and polymer B during melt processing. After the metering pumps, polymer melts A and B were combined in a custom designed three-layer coextrusion feedblock to form a three layer A/B/A structure. The three-layer polymer melt then flowed through a series of layer multiplier dies. In each of the multipliers, the number of layers in the polymer melt stream is doubled by a cutting, splitting, restacking process. For example, polymer melts with an A/B/A structure were split horizontally into two A/B/A melt flows, compressed in the vertical direction, and restacked and spread horizontally to form an A/B/A/B/A five layer structure after the first layer multiplier die. Additional layer multiplying dies placed in series will continue to sequentially cut, stack, and spread the polymer melt stream resulting in a final polymer melt that can be comprised of $2^{(n+1)}+1$ number of layers where n is the number of layer multiplying dies in series. A sacrificial skin layer of low density polyethylene (LDPE), which was later be removed prior to characterization or lens processing, was used to protect the films from dust as well as to minimize surface roughness during film coextrusion. Ultimately, the layered polymer melt was spread in a 350 mm wide film die and cast onto a heated, chrome polished rotating roll to a target thickness of 50 microns.

Utilizing this technique, polymer nanolayered films with 4097 layers were produced in four different systems including OKP4HT/PC, PC/SAN17, SAN 17/PMMA, and PMMA/PVDF-blend. The final film thickness (without sacrificial skin layer) of all systems was 50 μm. By targeting this film thickness with 4097 layers, the individual layer thickness of nanolayered film was below a quarter wave of visible light that results in a novel optical nanolayered film property of high optical transparency and volumetric composition controlled refractive index. The volume ratio of polymer A and polymer B in each system was maintained during processing by previously described melt metering pumps and varied in in 2% steps, so the respective volume ratio of PMMA/SAN17 were started from 100/0, 98/2 through 50/50 and ended with 0/100. Theoretically, the refractive index of polymer nanolayered films followed a volumetric compositional additive model and the volume compositions of each polymer system were selected to achieve a refractive index step size around 0.002.

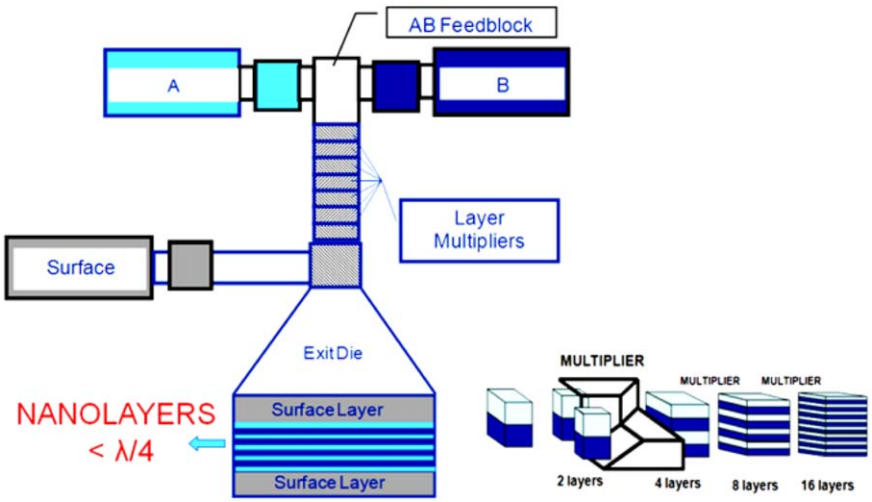

Figure 1. Multilayer coextrusion is able to produce nanolayer films with individual layer thickness below a quarter of the wavelength of visible light. [Color figure can be viewed in the online issue, which is available at wileyonlinelibrary.com.]

Polymer Nanolayer Film Characterization

The refractive index of the nanolayered films was measured using a 2010 Metricon prism-coupler equipped with a 633-nm laser. The measurement was carried out at room temperature. Polymer nanolayered film was push onto a prism with known refractive index under pressure. The laser beam passed through the prism and was normally totally reflected at the interface between the prism and the polymer film onto a detector. By rotating the laser beam, a critical angle was found as the reflected intensity of the laser beam dropped. The refractive index of polymer film can be calculated using critical angle based on Snell's law:[17]

$$n_{prism}\ \sin\theta_{prism} = n_{film}\ \sin\theta_{film} \quad (1)$$

where n is refractive index and θ is the angle. θ_{prism} is at critical angle, θ_{film} equaled 90° and refractive index of the film can be calculated.

Light transmission of the polymer nanolayered films was measured using an Ocean Optics SD 2000 fiber optic spectrometer. The spectrums were collect with wavelengths from 400 to 1000 nm.

Polymer GRIN Lens Fabrication

Polymer GRIN lenses were fabricated using the following procedure. A series of polymer nanolayered films were stacked and consolidated into a GRIN sheet. The refractive index distribution of the GRIN sheet can be controlled by selecting films with appropriate refractive index. One hundred polymer films with a controlled refractive index distribution were formed into a 5 mm stack. This film stack was then further consolidated to a GRIN sheet by compression molding. The thickness of the final GRIN sheet was 4 mm. Once the GRIN sheet was formed, a GRIN lens preform was fabricated using a compression molder with a concave ($R = 20.7$ mm) and a convex ($R = 18.1$ mm) spherical glass mold. A plano-convex GRIN lens was then fabricated by polishing the concave surface of the GRIN shell preform.

Polymer GRIN Lens Characterization

Attenuated total reflectance/Fourier transform infrared (ATR-FTIR, Nexus 870, Thermo Nicolet) microspectroscopy was used to characterize relative polymer composition at each point of the lenses and then used to calculate and confirm refractive index distribution. The microscope was equipped with a germanium crystal and an attenuated-total-reflectance slide-on attachment. The resolution of the spectra was 2 cm^{-1} (32 scans). The spectra were collected at 500 μm intervals along the diameter on the plano-surface of the lens. The sample area for each spectrum was 75 μm × 75 μm.

A two-pin-hole method was used with the following procedure to characterize focal length vs. aperture of the GRIN lens.[12] Collimated laser (633 nm) was transmitted through a series of two-pin-holes with a varying distance (d_1) from 0.5 to 16 mm. After passing through the pinholes, normally collimated laser beams were then focused through the GRIN lens and were projected on a screen. The focal length (f) as a function of lens aperture was calculated from d_1, d_2 and the distance from the lens to the screen (l) using the following equation:

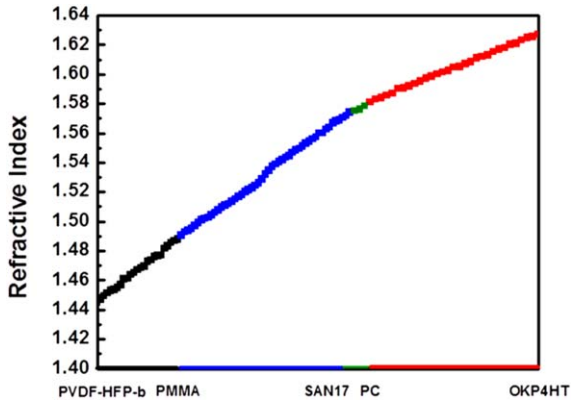

Figure 2. Refractive index of nanolayered films. [Color figure can be viewed in the online issue, which is available at wileyonlinelibrary.com.]

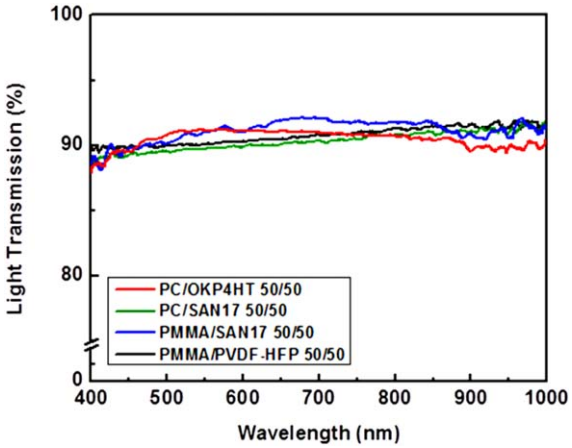

Figure 3. Light transmission of nanolayered films. [Color figure can be viewed in the online issue, which is available at wileyonlinelibrary.com.]

$$f = \frac{ld_1}{d_1 + d_2} \tag{2}$$

Optical form and figure of the GRIN lenses was characterized by surface interferometry at 633 nm using a Zygo Verifire Interferometer. Surface geometry was measured for all lenses with the optics resting vertically in a custom fabricated lens holder free of compressive mounts and stress. All measurements were conducted in a climate controlled environment kept at 22°C.

Dynamic mechanical thermal analysis (DMTA) was carried out using a DMA Q800 (TA Instruments) operating in a tensile mode. PMMA/SAN17 films were measured from 20°C to 130°C and PC/OKP4HT films were measured from 20°C to 170°C. Heating rate of DMTA test was 3°C/min and frequency was 1 Hz.

RESULTS AND DISCUSSION

Optical Properties of Polymer Nanolayered Films

The first step to fabricate a GRIN lens with the OKP4HT material involved characterizing optical properties of coextruded polymer nanolayered films to verify the composite film refractive index for building the GRIN distribution. The refractive index (R.I.) of the nanolayered films was measured using a prism coupling technique at room temperature with a laser wavelength of 633 nm. The R. I. of nanolayered films with a systematically varied the polymer composition against a compositional additive model[12] is described in the following equation:

$$n = n_1\phi_1 + n_2\phi_2 \tag{3}$$

where n is the total refractive index of the film. n_1 and n_2 are refractive indices of polymers and ϕ_1 and ϕ_2 are volume compositions of polymers. The refractive indices of OKP4HT (R.I.=1.63) /PC, PC/SAN17, SAN 17/PMMA, and PMMA/PVDF-blend films were plotted in Figure 2. As predicted for all the nanolayered film systems, the refractive indices of the films increased with increasing ratio of high refractive index components. Therefore, the refractive index range of the system was extended by introducing a high refractive index polymer OKP4HT.

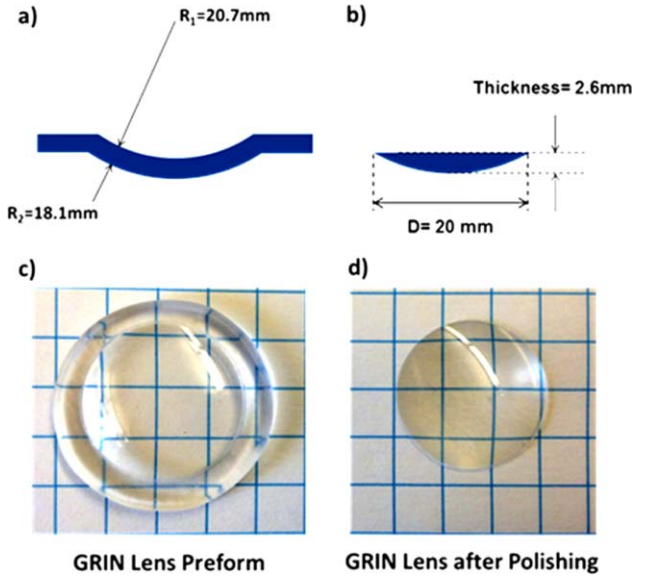

Figure 4. Design size (a, b) and images (c, d) of GRIN lens preform and GRIN lens after polishing. [Color figure can be viewed in the online issue, which is available at wileyonlinelibrary.com.]

In addition to the refractive index, light transmission is a key optical property for nanolayered films utilized to construct optics. The light transmission spectra of PC/OKP4HT, PC/SAN17, PMMA/SAN17, and PMMA/PVDF-b (50/50, v/v) was measured with UV/Vis spectrometer and plotted in Figure 3 from 400 to 1000 nm. For all nanolayered films, the film thickness was held constant at 50 μm at 4097 layers that result in an individual layer thickness at approximately 12 nm, which is below the quarter wavelength. At this layer thickness, there is no intrafilm light scattering at the nanometer scale layer interfaces. The resultant nanolayered films exhibited light transmission of about 90% irrespective of volumetric composition (value reported as uncompensated for the film-air surface losses).[18]

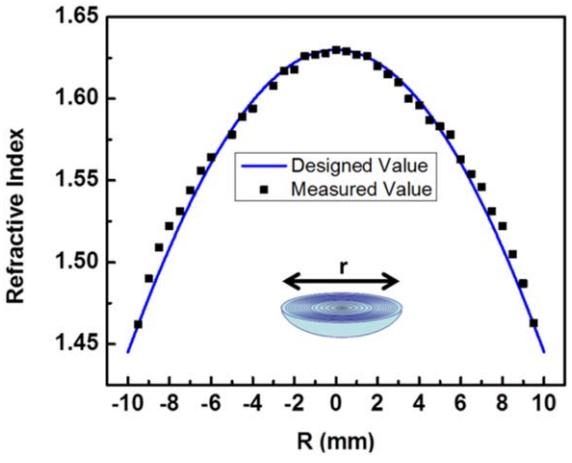

Figure 5. Refractive index distribution of $\Delta n = 0.185$ plano-convex GRIN lens. [Color figure can be viewed in the online issue, which is available at wileyonlinelibrary.com.]

Table II. Parameters of Plano-Convex High Δn GRIN Lens

	Materials	R. I.	R (mm)
OKP4HT Control	OKP4HT	1.63	20.7
$\Delta n = 0.05$	OKP4HT, PC	1.63-1.58	20.7
$\Delta n = 0.14$	OKP4HT, PC, PMMA, SAN17	1.63-1.49	20.7
$\Delta n = 0.185$	OKP4HT, PC, PMMA, SAN17, PVDF-HFP	1.63-1.445	20.7

Optical Performance of High Temperature GRIN Lens

Nanolayered films with an appropriate refractive index and light transmission were selected, physically stacked, and thermoformed against a pair of concave and convex spherical molds under vacuum and heat to produce a laminated GRIN preforms with a linear refractive index distribution through the thickness direction following processes previously described.[10] The laminated GRIN preform was polished on the concave surface to a plano-surface. The final geometry of the GRIN preform and GRIN lens were shown in Figure 4. The designed refractive index distribution could be achieved by choosing and stacking polymer nanolayered films with appropriate refractive indices. The refractive index distribution of the GRIN lens along the radius direction is described by the following equation:[19]

$$n(r) = n_{\max} - (n_{\max} - n_{\min}) \times \frac{\sqrt{r^2 + R_1^2} - R_0}{R_2 - R_1} \quad (4)$$

where $n_{\max}$ and $n_{\min}$ are the maximum and minimum refractive indices of the GRIN sheet/lens; R_2 and R_1 are the radii of the GRIN lens preform, which are 20.7 and 18.1 mm respectively; and r is the distance from the center of the lens to the measured point along the radius direction on the flat side of the lens. To characterize the refractive index profile of the GRIN lens, the composition of the polymer pairs along the radius direction was measured by ATR-FTIR microspectroscopy. The polymer composition at a certain point was determined from normalized peak intensity for OKP4HT at 1721 cm^{-1}, PC at 1772 cm^{-1}, SAN17 at 698 cm^{-1}, PMMA at 1727 cm^{-1}, and PVDF-HFP at 876 cm^{-1}.[19] The refractive index of the measured point was calculated from the composition of the polymers. The predicted and ATR-FTIR-measured refractive index distributions of a GRIN lens with a $\Delta n = 0.185$, were plotted in Figure 5. The refractive index distribution of the GRIN lens matched the expected design profile.

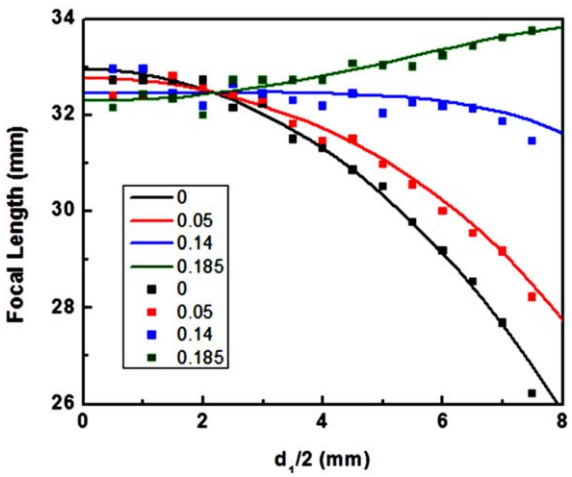

Figure 6. Spherical aberration correction of lens with varying GRIN lens Δn. [Color figure can be viewed in the online issue, which is available at wileyonlinelibrary.com.]

In order to characterize the optical performance of a high temperature GRIN lens with extended Δn range, a series of GRIN lenses with a Δn up to 0.185 were produced (Table II). An OKP4HT homogeneous lens was also fabricated with the same geometry as the control lens. The GRIN lens focal length is attributed by a combination of optical power contributions, curvature, and internal optic refractive index distribution. The power contribution of lens curvature can be calculated from lens maker's equation, the following equation:

$$\frac{1}{f} = (n-1)\left[\frac{1}{R_1} - \frac{1}{R_2} + \frac{(n-1)d}{nR_1R_2}\right] \quad (5)$$

where f is the focal length of the lens, and n is the refractive index of the lens material. R_1 and R_2 are radii of curvature of the lens, and d is the thickness of the lens. Additionally, the contribution of the refractive index distribution can be obtained analytically from the focusing power of a GRIN medium with a parabolic refractive index gradient as discussed in a previous work.[6] After combining the effects of the curvature and refractive index distribution, the focal length (f) dependence on position of the lens (r) of the GRIN lens can be described by the following equation:

$$\frac{1}{f} = \frac{2(n_{\max} - n_{\min})}{R_2^2 - R_1^2}\left(\sqrt{R_2^2 - r^2} - R_1\right)\left(\sqrt{R_2^2 - r^2} + \frac{R}{\tan\left(\arcsin\left((r * n_{\min}/R_2 * n_{air}) - \arcsin\left(r/R_2\right)\right)\right)} - R_2\right)^{-1} \quad (6)$$

where n_{max} and n_{min} are the maximum and minimum refractive indices and n_{air} is the refractive index of air. R_1 and R_2 are radii of the GRIN lens perform, and r is the half lens aperture. For the OKP4HT control lens, n_{max} is equal to n_{min}. Therefore, the

Table III. Parameters of PC/OKP4HT and PMMA/SAN17 GRIN Lens

System	Materials	R. I.	R (mm)
#1	OKP4HT, PC	1.63-1.58	20.7
#2	PMMA, SAN17	1.57-1.49	20.7

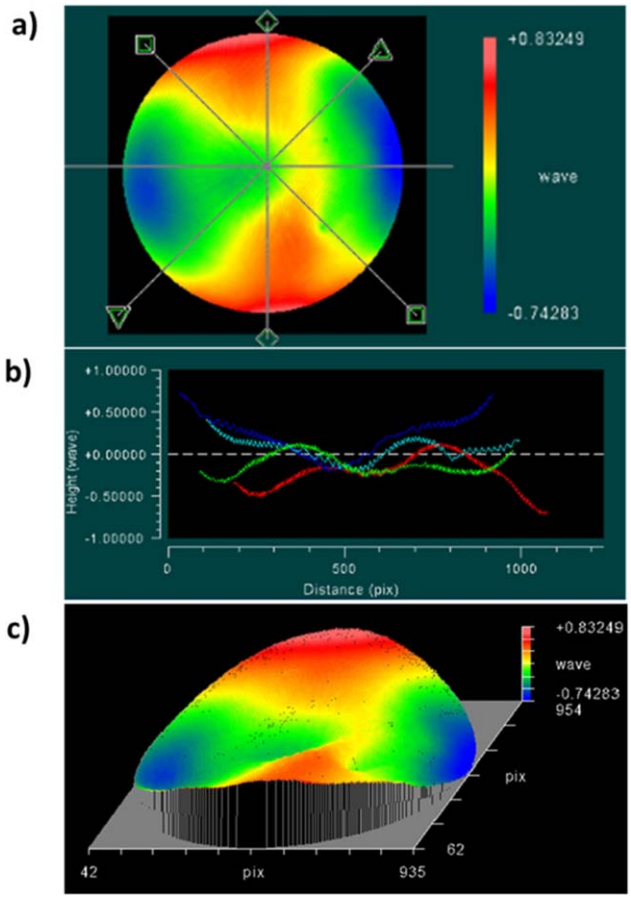

Figure 7. Optical figure of GRIN lens characterized by surface interferometry. [Color figure can be viewed in the online issue, which is available at wileyonlinelibrary.com.]

focal length equation of the OKP4HT control lens can be simplified[12] to the following equation:

$$\frac{1}{f}=\left(\sqrt{R_2^2-r^2}+\frac{R}{\tan\left(\arcsin\left((r*n_{\min}/R_2*n_{air})-\arcsin\left(r/R_2\right)\right)\right.}-R_2\right)^{-1} \quad (7)$$

Spherical aberration can be defined as the focal length difference between the center and the edge of the lens. To characterize the spherical aberration correction of a series of GRIN lenses ($\Delta n = 0.05$, 0.14, and 0.185) and an OKP4HT lens, the focal length as a function of aperture of lens (r) is measured against this analytical prediction using the two-pin-hole method.[19] The focal length vs. aperture results for the GRIN lens and OKP4HT homogenous lenses were plotted in Figure 6. As expected because of the larger optical path length, a homogeneous lens focal length at small aperture was larger than on the edges. A series of increasing Δn of the GRIN optics resulted in a dramatically smaller difference in the focal length between the small and large apertures. The GRIN lens with $\Delta n = 0.185$ even exhibited over correction, that resulted in a reversing of the spherical aberration. This demonstrates the ability to design a GRIN lenses with an ability to correct spherical aberrations. Therefore, an optical imaging system with better optical power can be designed and produced by achieving a high Δn GRIN system with a high temperature polymer (OKPH4T). Additionally, the optical system can be lighter and less complex with a higher Δn GRIN system.

Temperature Survival Performance

High temperature polymer, OKP4HT, not only increases the refractive index range of the GRIN system, but also improves the temperature survival performance. In order to investigate the effect of a high temperature polymer, OKP4HT, on the temperature survival performance of the GRIN system, two polymer GRIN lens systems were fabricated using PMMA/SAN17 and PC/OKP4HT, with the parameters listed in Table III. The 3D surface topography of an initial GRIN lens was measured using a Zygo interferometer equipped with a diode laser (λ=633 nm). The molded convex surface of the OKP4HT/PC GRIN lens was measured interferometrically, Figure 7, as a reference prior to the thermal treatment. In this image, the red regions corresponded to a measured radius larger (+ deviation) than the designed value (20.7 mm) and the blue regions corresponded to a measured radius less (− deviation) than the designed value. The maximum positive deviation is 0.83 waves or 529 nm (0.83 × 633 nm), while the maximum negative deviation is 468.42 nm. The deviation along the lines drawn in Figure 7(a) are plotted in Figure 7(b), and across all the points the deviation was always within 1 wave (<633 nm). The 3D deviation profile of the GRIN lens is shown in Figure 7(c), and demonstrates that the measured 3D profile matched that of the designed value. The shape of a second PMMA/SAN17 GRIN lens was also measured and found to follow the designed value.

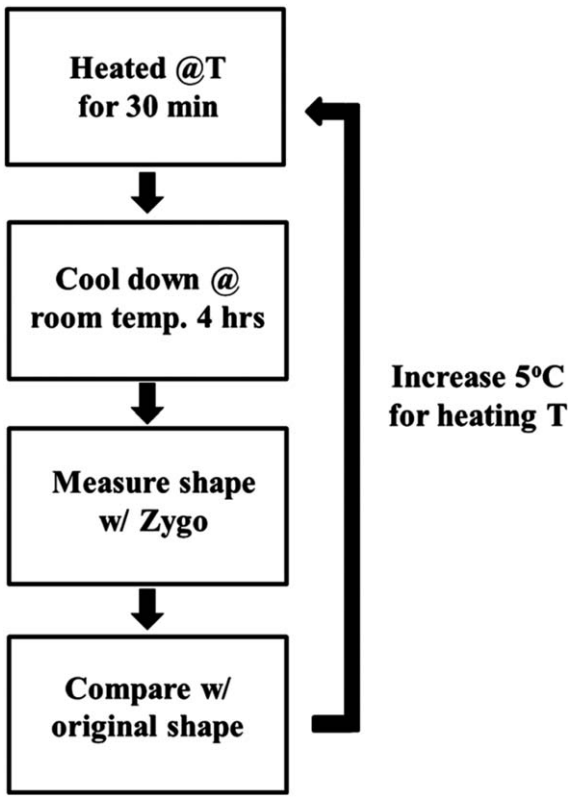

Figure 8. Protocol to determine upper service temperature (UST).

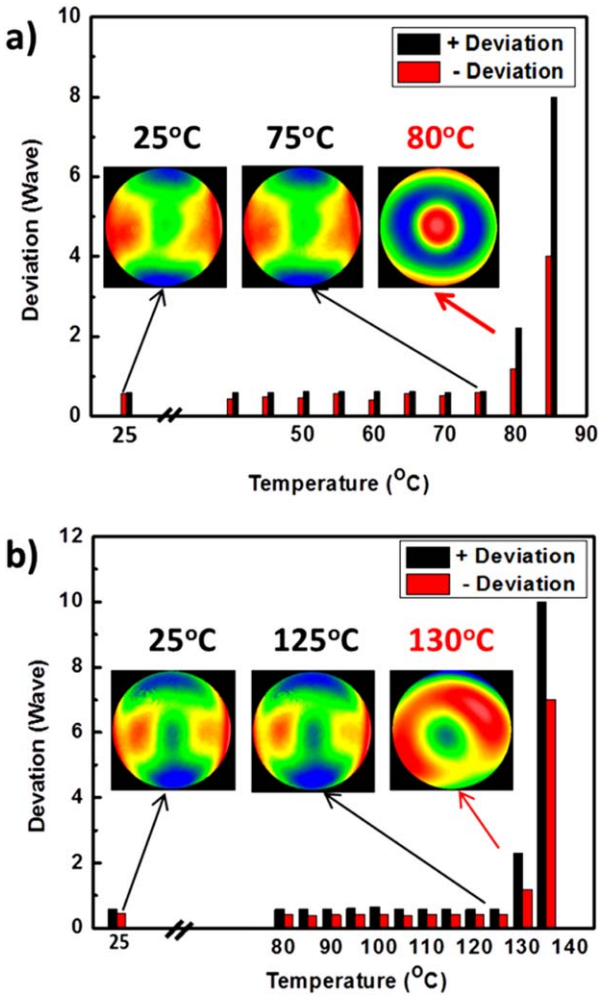

Figure 9. Shape change vs. temperature of (a) PMMA/SAN17 GRIN lens, (b) OKP4HT/PC GRIN lens. [Color figure can be viewed in the online issue, which is available at wileyonlinelibrary.com.]

Polymeric GRIN lens upper service temperature (UST) and thermal hysteresis effects on PMMA/SAN17 GRIN lenses were characterized using the following procedure, Figure 8. A PMMA/SAN17 GRIN lens was heated in an oven at 30°C for 30 minutes and then cooled down to room temperature over a 4 hour period to ensure internal optic temperature equilibrium prior to interferometric measurements. The convex surface of the lens was measured using Zygo interferometer. The measured shape after heating was compared with original shape of the lens measured at room temperature (25°C). After this, the lens was again heated in the oven at 5°C higher temperatures (35°C) and all the previous steps will be repeated to determine if permanent optic shape changes resulted. Thermal exposures to increasingly higher temperatures were repeated following the previously described procedure up to the glass transition temperature of the highest nanolayered film polymer material.

The ultimate degree of GRIN optic convex surface radius change was determined by a comparison of the maximum radius deviation from the initial, room temperature, value. The radius deviation of the PMMA/SAN17 GRIN lens was plotted in Figure 9(a). The positive and negative deviations of the PMMA/SAN17 GRIN lens were approximately 0.5 waves after heating from room temperature up to 75°C. These values doubled at 80°C and increased dramatically at 85°C. The 2D deviation profile [Figure 9(a) insert] of the PMMA/SAN17 GRIN lens also changed significantly when the temperature reached 80°C. These data suggested that the shape/optical properties of the lens will not be significantly changed by heating with temperature up to 75°C. Therefore, the UST of PMMA/SAN17 system was designated to be 75°C.

Motivated by the need for an optical system with a higher upper service temperature (UST) than that of the PMMA/SAN17 system, a second polymer nanolayered system, PC/OKP4HT, was developed. The UST of the PC/OKP4HT GRIN lens was determined using the same method as discussed previously. The interferometric figure of the PC/OKP4HT GRIN lens was plotted in Figure 9(b). The positive deviation of the PC/OKPH4T GRIN lens increased from 0.5 waves to 2 waves and the negative deviation increased from 0.5 waves to 1 wave at 130°C, while the 2D radius deviation profile [Figure 9(b) insert] showed similar changes. Therefore, the UST of OKP4HT/PC system was assigned at 125°C which is 50°C higher than PMMA/SAN17 system.

The relation of the UST to the T_gs of homogeneous polymer materials as well as 50/50 nanolayered films was characterized using DMTA. For the PMMA/SAN17 system, T_g of PMMA and SAN17 were 99°C and 104°C, which were determined by loss modulus peak of each polymer (Table IV). A 4097 layer PMMA/SAN17 film (50/50 v/v) had a single T_g at 102°C, which represents agreement to a compositional dependent average T_g of the two homogeneous materials. The T_g of OKP4HT/PC system followed the similar trend. 4097 layer of PC/ OKP4HT film (50/50 v/v) had a T_g of 145°C, which was approximately the average T_g of PC (147°C) and OKP4HT (142°C). Based on previous research,[20] when two compatible polymers were layered against each other, an "interphase region" was created. The T_g shifted closer together with decreasing layer thickness. When the individual layer thickness was less than the interphase thickness of the two materials, a single T_g was exhibited for compatible polymer nanolayered films with thousands of layers. The merged T_g can be predicted by the volume ratio of the two polymers based on the following equation:

$$T_{g,i} = V_A T_{g,A} + V_B T_{g,B} \quad (8)$$

where $T_{g,i}$ is the glass transition temperature of the nanolayered films, $T_{g,A}$ and $T_{g,B}$ are the glass transition temperatures of the

Table IV. Glass Transition Temperature of GRIN Films

Comp.	T_g (°C)
PMMA	99
PMMA/SAN17 50/50	102
SAN17	104
OKP4HT	142
OKP4HT/PC 50/50	145
PC	147

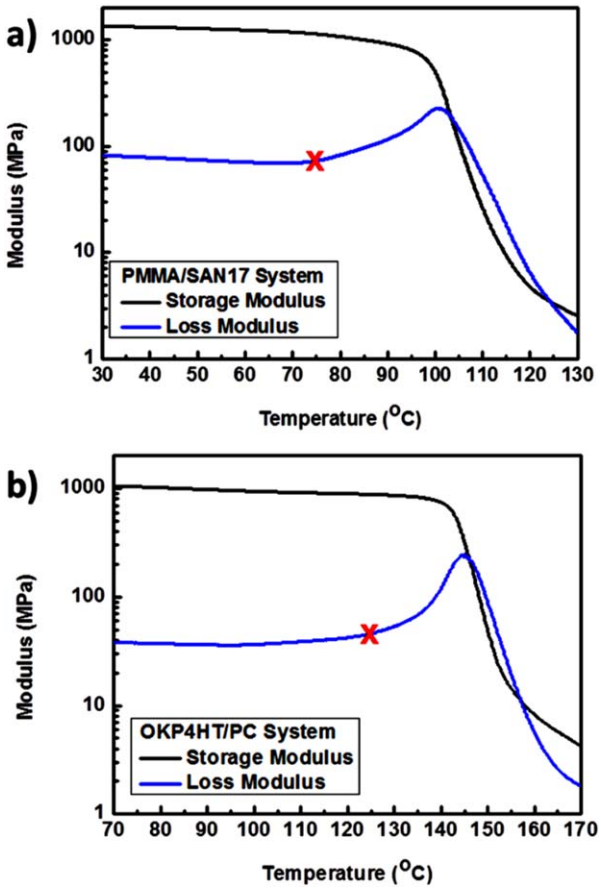

Figure 10. DMA of (a) PMMA/SAN17 system, (b) PC/OKP4HT system. [Color figure can be viewed in the online issue, which is available at wileyonlinelibrary.com.]

two materials, and V_A and V_B are the mass ratio of the two materials. The glass transition temperatures of PMMA/SAN17 and PC/OKP4HT films (50/50 v/v) followed the prediction based on this equation. The modulus and loss modulus of PMMA/SAN17 and PC/OKP4HT film (50/50 v/v) vs. temperature were measured (Figure 10) to correlate UST to glass transition temperature of polymer nanolayered films. Based on the temperature survival performance study, the shape of PMMA/SAN17 lens began to change at 80°C which was corresponded to the onset of the loss modulus peak of the PMMA/SAN17 (50/50 v/v) films. The OKP4HT/PC GRIN lens exhibited a similar trend. There is greater chain mobility and the system becomes more susceptible to creep after the temperature is higher than the onset of the loss modulus peak, which accounts for the measured deformation of the lenses upon heating. By introducing a high temperature polymer system (PC/OKP4HT), polymer chain mobility changed to higher temperature with an increased T_g compared with PMMA/SAN17 system. The upper service temperature of GRIN lens with polymer nanolayered materials was extended 50°C through developing a higher temperature polymer nanolayered system with OKP4HT.

CONCLUSION

A high temperature polymer, OKP4HT, was involved in developing new polymer nanolayered GRIN systems. Nanolayered films for new polymer GRIN system were coextruded with five different polymers including OKP4HT, PC, SAN17, PMMA, and PVDF-b. The refractive index of the films followed a compositional additive model and increase with increasing ratio of high refractive index polymer. The new polymer nanolayered GRIN system exhibited a higher refractive range of 0.185 without sacrificing light transmission of individual films. A series of GRIN lenses with Δn from 0 to 0.185 were produced in order to study the optical performance. Refractive index distribution of polymer GRIN lens was confirmed by calculation from composition of the polymers at each position of the lens. The refractive index distribution was found to match the expected designed profile. The GRIN lens with higher Δn value exhibited better spherical aberration correction based on focal length vs. aperture measurement. The GRIN lens with $\Delta n = 0.185$ even showed an over correction. Therefore, a polymer GRIN system with high refractive index range will provide better optical power and more flexibility for optical system design and manufacture, which potentially may also decrease the weight and complexity of the optical system. The polymer GRIN system involved OKP4HT can not only increase Δn of the system but also enhance temperature survival performance of the polymer GRIN system. UST of PMMA/SAN17 system and PC/OKP4HT system was determined by thermal cycle of the lens followed with interferometric measurement of shape change vs. temperature. The UST of OKP4HT/PC system was determined to by 125°C, 50°C higher than PMM/SAN17 system, which means the polymer GRIN system will have a better temperature survival performance by involving high temperature polymer, OKP4HT. The temperature survival performance of polymer nanolayered system correlated with the onset of the material loss modulus as measured by material thermal-mechanical testing. Even in a nanolayered state, composite polymer nanolayered films exhibited a single film T_g that followed an volumetric average of the film constituent polymer materials. Optical polymer material systems, even fabricated from thousands of nanolayers, appear to follow an UST predictable by its onset of loss modulus peak.

ACKNOWLEDGMENTS

This project was conducted with the generous financial support of the National Science Foundation Science and Technology Center, Center for Layered Polymeric Systems (DMR-0423914) and the Defense Advanced Research Projects Agency (DARPA) (HR0011-04-C-0043). The authors thank Curtis Whalen for their careful reading and improving the manuscript.

REFERENCES

1. Doushkina, V.; Fleming, E. Proceedings of SPIE Optical Engineering, San Diego, USA, August 2, **2009**.
2. Sun, L.; Kim, J. H.; Jang, C. H.; An, D.; Lu, X.; Zhou, Q.; Taboada, J. M.; Chen, R. T.; Maki, J. J.; Tang, S.; Zhang, H.; Steier, W. H.; Zhang, C. H.; Dalton, L. R. *Opt. Eng.* **2001**, *40*, 1217.

3. Song, H.; Singer, K.; Lott, J.; Wu, Y.; Zhou, J.; Andrews, J.; Baer, E.; Hiltner, A.; Weder, C. *J. Mater. Chem.* **2009**, *19*, 7520.
4. Kuswandi, B.; Huskens, J.; Verboom, W. *Anal. Chim. Acta* **2007**, *601*, 141.
5. Sultanova, N. G.; Kasarova, S. N.; Nikolov, I. D. *J. Phys. Conf. Ser.* **2012**, *398*, 012030.
6. Peters, K. *Smart Mater. Struct.* **2011**, *20*, 3002.
7. Eldada, L.; Shacklette, L. W. *IEEE J. Sel. Top. Quantum Electron.* **2000**, *6*, 54.
8. Liu, J. G.; Ueda, M. *J. Mater. Chem.* **2009**, *19*, 8907.
9. Mariko, K.; Ito, Hiroshi. *J. Polym. Eng.* **2013**,*33*, 557.
10. Baer, E.; Hiltner, P. A.; Shirk, J. S. (Case Western Reserve University). U.S. Patent 7,002,754, B2, February 21, **2006**.
11. Ponting, M.; Fein, H. Optical Fabrication and Testing. Optical Society of America, Kohala Coast, USA, Jun 22, **2014**.
12. Ji, S.; Yin, K.; Mackey, M.; Brister, A.; Ponting, M.; Baer, E. *Opt. Eng.* **2013**, *52*, 112105.
13. Meemon, P.; Yao, J.; Lee, K. S.; Thompson, K. P.; Ponting, M.; Baer, E.; Rolland, J. P. *Sci. Rep.* **2013**, *3*, 1.
14. Ji, S.; Ponting, M.; Lepkowicz, R. S.; Rosenberg, A.; Flynn, R.; Beadie, G.; Baer, E. *Opt. Express.* **2012**, *20*, 26746.
15. Liu, R. Y. F.; Bernal-Lara, T. E.; Hiltner, A.; Baer, E. *Macromolecules* **2005**, *38*, 4819.
16. Ponting, M.; Hiltner, A.; Baer, E. *Macromol. Symp.* **2010**, *294*, 19.
17. Metricon operation manual.
18. Lai, C. Y.; Ponting, M.; Baer, E. *Polymer* **2012**, *53*, 1393.
19. Jin, Y.; Tai, H.; Hiltner, A.; Baer, E. *J. Appl. Polym. Sci.* **2007**, *103*, 1834.
20. Liu, R. Y. F.; Ranade, A. P.; Wang, H. P.; Bernal-Lara, T. E.; Hiltner, A.; Baer, E. *Macromolecules* **2005**, *38*, 10721.